J Antimicrob Chemother 2014; **69**: 2759–2769
doi:10.1093/jac/dku183 Advance Access publication 7 June 2014

Journal of Antimicrobial Chemotherapy

The M-T hook structure increases the potency of HIV-1 fusion inhibitor sifuvirtide and overcomes drug resistance

Huihui Chong[1]†, Xue Yao[1]†, Zonglin Qiu[1]†, Jianping Sun[1]†, Yuanyuan Qiao[1], Meng Zhang[1], Meitian Wang[2], Sheng Cui[1]‡ and Yuxian He[1]*‡

[1]*MOH Key Laboratory of Systems Biology of Pathogens and AIDS Research Center, Institute of Pathogen Biology, Chinese Academy of Medical Sciences & Peking Union Medical College, Beijing 100730, China;* [2]*Swiss Light Source, Paul Scherrer Institute, CH-5232 Villigen, Switzerland*

*Corresponding author. Tel: +86-10-67870275; Fax: +86-10-67870275; E-mail: yhe@ipb.pumc.edu.cn
†These authors contributed equally to this work.
‡These authors contributed equally to this work.

Received 11 March 2014; returned 10 April 2014; revised 29 April 2014; accepted 1 May 2014

Objectives: Peptides derived from the C-terminal heptad repeat (CHR) of HIV-1 gp41 are potent fusion inhibitors. We have recently demonstrated that the unique M-T hook structure preceding the pocket-binding motif of CHR peptide-based inhibitors can greatly improve their antiviral activity. In this study, we applied the M-T hook structure to optimize sifuvirtide (SFT), a potent CHR-derived inhibitor currently under Phase III clinical trials in China.

Methods: The peptide MT-SFT was generated by incorporating two M-T hook residues (Met-Thr) into the N-terminus of sifuvirtide. Multiple structural and functional approaches were used to determine the biophysical properties and antiviral activity of MT-SFT.

Results: The high-resolution crystal structure of MT-SFT reveals a highly conserved M-T hook conformation. Compared with sifuvirtide, MT-SFT exhibited a significant improvement in the ability to bind to the N-terminal heptad repeat, to block the formation of the six helix bundle and to inhibit HIV-1 Env-mediated cell fusion, viral entry and infection. Importantly, MT-SFT was fully active against sifuvirtide- and enfuvirtide (T20)-resistant HIV-1 variants and displayed a high genetic barrier to developing drug resistance.

Conclusions: Our studies have verified that the M-T hook structure offers a general strategy for designing novel HIV-1 fusion inhibitors and provide new insights into viral entry and inhibition.

Keywords: HIV gp41, six-helix bundle, peptide inhibitors, genetic barrier

Introduction

More than 60 million people have been infected by HIV-1 and ~25 million people have died of AIDS-related diseases (www.unaids.org). Six classes of HIV-1 inhibitors in clinics are directed against four specific steps of the viral life cycle, including cell entry, reverse transcription, integration and virion maturation.[1,2] Different from other classes of anti-HIV drugs that act after infection occurs, HIV-1 entry inhibitors intercept the virus before it invades the target cells.[3,4] Currently, there are two HIV-1 entry inhibitors for clinical use: maraviroc (UK-427857), approved in 2007, binds to the cell coreceptor CCR5 thus blocking the binding of virus;[5,6] and enfuvirtide (T20), a 36 amino acid peptide derived from the C-terminal heptad repeat (CHR) region of HIV-1 transmembrane protein gp41 (Figure 1), binds to the N-terminal heptad repeat (NHR) region of gp41 thus preventing the formation of viral fusion core, the gp41 six helix bundle (6-HB).[7–9] Approved in April 2003, enfuvirtide is the first and only fusion inhibitor used in combination therapy of HIV-1 infection. However, enfuvirtide requires high dosages and drug resistance is easily acquired,[10–13] calling for a next generation of HIV-1 fusion inhibitors.

A series of novel HIV-1 fusion inhibitors have been created by using the CHR-derived peptide C34 as a template.[14–16] The rationale is based on the following: (i) the protease-resistant C34 was used to determine the first gp41 structure (6-HB), thus representing a core sequence of the CHR;[17,18] (ii) C34 contains the NHR pocket-binding motif at its extreme N-terminus, thus stabilizing the interaction of inhibitor with the target site;[17,19,20] and (iii) C34 has higher potency than enfuvirtide to inhibit both wild-type and enfuvirtide-resistant HIV-1 isolates.[13,16,21] Based on the three-dimensional structure of gp41, sifuvirtide (SFT) was designed by introducing multiple salt bridges into C34 and further incorporating a serine residue into its N-terminus.[22] Compared with its parental peptide, sifuvirtide exhibited significantly improved antiviral activity

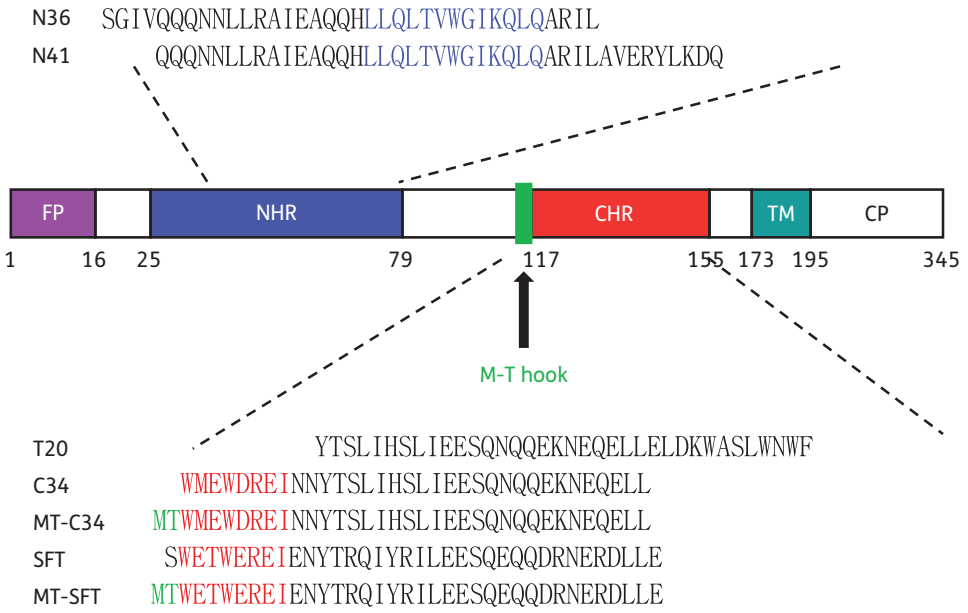

Figure 1. Schematic illustration of the HIV-1 gp41 functional domains and the sequences of NHR- or CHR-derived peptides. The gp41 numbering of HIV-1_{HXB2} is used. FP, fusion peptide; TM, transmembrane domain; CP, cytoplasmic tail. The sequences corresponding to the NHR pocket region are shown in blue. The sequences corresponding to the CHR pocket-binding domain are shown in red. The position and sequence for the M-T hook structure are shown in green.

and pharmaceutical profiles.[22] Our crystallographic studies have provided the structural basis for sifuvirtide, confirming the original design strategy of the peptide and revealing the key motifs responsible for its stability and antiviral activity.[23] Indeed, several novel interhelix salt bridges and hydrogen bonds improve the binding affinity of sifuvirtide for the target NHR region and the extra serine residue stabilizes the N-terminal portion of the peptide.[23] Sifuvirtide has already been advanced into clinical Phase III trials in China. However, it was also found that sifuvirtide had a relatively low genetic barrier to induction of drug resistance.[24] In *in vitro* selection, a panel of sifuvirtide-resistant HIV-1 variants could be easily obtained.[24] Similar to enfuvirtide, the responsible mutations of sifuvirtide resistance were largely mapped to the inhibitor binding sites in the NHR, which overlapped with enfuvirtide-resistant mutations either singly or in combination, such as I37T, V38A, N43K and I37T/N43K (according to HIV-1_{HXB2} gp41 numbering throughout).[10–12] Therefore, new strategies or concepts are eagerly wanted to develop HIV-1 fusion inhibitors that not only inhibit the existing resistant HIV-1 variants but also possess high genetic barriers to induction of drug resistance.

We previously identified that the CHR-derived peptide CP32 (i.e. CP621-652) had a much higher binding affinity than C34 for the NHR target.[25] Following that we designed CP32M, which exhibited a significantly improved anti-HIV activity especially against enfuvirtide-resistant viruses.[26] Recently, we determined the crystal structure of CP32 and identified that the residues Met115 and Thr116 preceding the pocket-binding domain (PBD) of the peptide forms a hook-like structure, named the M-T hook.[27] We also demonstrated that addition of the M-T hook structure to the N-termini of C34 or the short peptide SC22EK could greatly increase the binding affinity and antiviral activity of the inhibitors,[28,29] addressing the importance of the M-T hook as a vital strategy to design or optimize HIV-1 fusion inhibitors. In this study, we engineered sifuvirtide by adding the M-T hook to improve its pharmaceutical profiles. The high-resolution crystal structures confirmed the M-T hook conformation presented at the N-terminus of sifuvirtide. We demonstrated that the M-T hook structure markedly enhanced the binding affinity and anti-HIV activity of sifuvirtide, especially against those sifuvirtide- and enfuvirtide-resistant HIV-1 mutants. Significantly, the resulting peptide (MT-SFT) had an increased genetic barrier compared with sifuvirtide to the development of resistance.

Materials and methods

Peptide synthesis

The CHR-derived peptides enfuvirtide, sifuvirtide, MT-SFT, C34 and MT-C34 and the NHR-derived peptides N41, N36 and N36 mutants (I37T, V38A, Q40H, N43K, I37T/N43K and V38A/N42T) were synthesized by a standard solid-phase Fmoc method as described previously.[28] All peptides were acetylated at the N-terminus and amidated at the C-terminus. They were purified by reversed-phase HPLC and verified for purity >95% and correct amino acid composition by mass spectrometry. The concentrations of the peptides were determined by UV absorbance and a theoretically calculated molar extinction coefficient ε (280 nm) of 5500 and 1490 M^{-1} cm^{-1} based on the number of tryptophan and tyrosine residues, respectively.

Structure determination of the 6-HB-containing MT-SFT

In order to determine the crystal structure of 6-HBs formed by MT-SFT/N36 and MT-SFT/N41, MT-SFT peptide and its NHR counterparts (N36 or N41), synthetic peptides MT-SFT/N36 or MT-SFT/N41 were mixed at 1:1 molar ratio and were dissolved in denaturing buffer containing 100 mM NaH_2PO_4, 10 mM Tris HCl pH 8.0 and 8 M urea, respectively. The refolding was carried out by dialysis against refolding buffer containing 50 mM Tris-HCl (pH 7.5), 100 mM NaCl at 4°C overnight, yielding soluble 6-HBs. The 6-HBs were finally purified by size-exclusion chromatography

(Superdex 75 10/300 GL, GE Healthcare). A predominant peak corresponding to the size of the 6-HB was collected and concentrated prior to crystallization trials. The 6-HB composed of MT-SFT/N36 was crystallized by mixing equal volumes (1 μL) of the concentrated sample (~10 mg/mL) and reservoir solution containing 0.14 M calcium chloride, 0.1 M sodium acetate (pH 4.6) and 18% (v/v) 2-propanol at 22°C. The cryocooling was carried out by soaking the crystals for 60 s in reservoir solution containing 15% glycerol followed by flash freezing in liquid nitrogen. The 6-HB composed of MT-SFT/N41 was crystallized by mixing equal volumes (1 μL) of purified sample (~10 mg/mL) and reservoir solution containing 0.1 M MES buffer pH 6.4, 26% (v/v) PEG 4000 in a hanging drop vapour diffusion system at 22°C. The cryocooling was carried out by soaking the crystals for 40 s in reservoir solution containing 15% glycerol followed by flash freezing in liquid nitrogen. Complete datasets for the MT-SFT/N36 and MT-SFT/N41 complexes were collected at beamline X10SA, Swiss Light Source at Paul Scherrer Institute using X-rays with a wavelength of 1.000 Å. The crystal structure containing MT-SFT/N36 and MT-SFT/N41 was solved by molecular replacement (Phaser for MR, CCP4 package) using the crystal structure of sifuvirtide (PDB ID: 3VIE) as the searching models, which yielded the interpretable electron-density maps. Both structures were refined (PHENIX) to finalize the atomic models with excellent refinement statistics and stereochemical qualities and validated by MolProbity analysis (Table S1, available as Supplementary data at *JAC* Online). The MolProbity scores for the crystal structures of the 6-HBs containing MT-SFT/N36 and MT-SFT/N41 are 1.37 and 1.24, rating 93rd and 96th percentiles among structures of comparable resolution, respectively. The Ramachandran plots of both structures find all residues in the favoured area.

Circular dichroism (CD) spectroscopy

CD spectroscopy was performed according to the protocol described previously.[30] Briefly, a CHR peptide (C34, SFT or MT-SFT) was incubated with an equal molar concentration of NHR peptide N36 or its mutant (I37T, V38A, Q40H, N43K, I37T/N43K and V38A/N42T) at 37°C for 30 min. The final concentration of each peptide was 10 μM in PBS buffer (pH 7.2). The CD spectra were acquired on a Jasco spectropolarimeter (model J-815) using a 1 nm bandwidth with a 1 nm step resolution from 195 to 260 nm at room temperature. The spectra were corrected by subtraction of a blank corresponding to the solvent. The data were averaged over three accumulations. The α-helical content was calculated from the CD signal by dividing the mean residue ellipticity [θ] at 222 nm by the value expected for 100% helix formation ($-33\,000$ degrees.cm^2.dmol^{-1}). The thermal denaturation was performed by monitoring the ellipticity [θ] at 222 nm from 20–98°C using a temperature controller. The temperature was increased at a rate of 1.2°C/min; data were acquired at a 1 nm bandwidth at 222 nm at a frequency of 0.25 Hz. The melting curve was smoothed and the midpoint of the thermal unfolding transition (T_m) values was taken as the maximum of the derivative d[θ]$_{222}$/dT. The T_m value was detected at a peptide concentration of 10 μM in PBS buffer.

Isothermal titration calorimetry (ITC)

ITC assay was performed using an iTC200 microcalorimeter instrument (MicroCal, USA) as described previously.[28] Briefly, 1 mM N36 dissolved in double-distilled H_2O (ddH_2O) was injected into the chamber containing 100 μM sifuvirtide or MT-SFT. The experiments were carried out at 25°C. The time between injections was 240 s and the stirring speed was 500 rpm. The heats of dilution were determined in control experiments by injecting N36 into ddH_2O and subtracted from the heats produced in the corresponding peptide–peptide binding experiments. Data acquisition and analysis were performed using MicroCal Origin software (version 7.0).

Cell–cell fusion assays

293T effector cells seeded in six-well plates at 4×10^5 cells/well were transfected with the plasmid encoding HIV-1_{NL4-3} Env. The day after transfection, the effector cells were incubated with MT-4 cells at a ratio of 1:3 in 96-well plates in the presence or absence of tested peptides. After coculturing for an additional 48 h at 37°C, the syncytia of each well were counted under a microscope. The percentage inhibition of fusion by the peptides and 50% inhibitory concentration (IC_{50}) values of fusion were calculated using GraphPad Prism software (GraphPad Software Inc., San Diego, CA, USA).

HIV-1 single-cycle infection

HIV-1 pseudoviruses were generated as described previously.[31] Briefly, 293T cells were co-transfected with an Env-expressing plasmid and a backbone plasmid pSG3$^{\Delta env}$ that encodes Env-defective, luciferase-expressing HIV-1 genome using Lipofectamine 2000 reagent (Invitrogen). Pseudovirus-containing culture supernatants were harvested 48 h after transfection and filtered using a 0.45 μm pore size. The 50% tissue culture infectious dose ($TCID_{50}$) of the pseudovirus was determined in TZM-bl cells. The inhibitory activity of sifuvirtide and MT-SFT was determined using TZM-bl cells. Briefly, the peptides were prepared with 10 series dilutions in a 3-fold stepwise manner and mixed with 100 $TCID_{50}$ viruses and incubated for 1 h at room temperature. The mixture was added to TZM-bl cells (10^4/well) and incubated at 37°C for 48 h before the luciferase activity was measured as described previously.[31]

Inhibition of HIV-1_{NL4-3} infection

The molecular clone of wild-type or drug-resistant HIV-1_{NL4-3} was prepared by transfection of pNL4-3 plasmid into 293T cells. The virus stock was harvested 48 h post-transfection and quantified for $TCID_{50}$. Inhibition of infection by sifuvirtide and MT-SFT on HIV-1_{NL4-3} was performed as described for pseudovirus. Briefly, 100 $TCID_{50}$ viruses were used to infect TZM-bl cells in the presence or absence of serially diluted peptides. Two days post-infection, the cells were harvested and lysed in reporter lysis buffer and the luciferase activity was measured.

Inhibition of 6-HB formation by peptides

A mouse monoclonal antibody specific for the gp41 6-HB (NC-1) was obtained from Dr Shibo Jiang through the AIDS Research and Reference Reagent Program, Division of AIDS, NIAID, National Institutes of Health. The inhibitory activity of CHR peptides on the 6-HB formation was measured by a modified ELISA-based method as described previously.[30] Briefly, a 96-well polystyrene plate (Costar, Corning Inc., Corning, NY, USA) was coated with NC-1 (2 μg/mL in 0.1 M Tris, pH 8.8). A tested peptide (sifuvirtide or MT-SFT) at graded concentrations was mixed with C34-biotin (0.1 μM) and incubated with N36 (0.1 μM) at room temperature for 30 min. The mixture was then added to the NC-1-coated plate, followed by incubation at room temperature for 30 min and washing with a washing buffer (PBS containing 0.1% Tween 20) three times. Then, horseradish peroxidase-labelled streptavidin (Invitrogen) and the substrate 3,3,5,5-tetramethylbenzidine (Sigma) were added sequentially. Absorbance at 450 nm was measured using an ELISA reader (Bio-Rad).

Induction of inhibitor-resistant HIV-1 variants

The *in vitro* selection of peptide inhibitor-resistant HIV-1 variants was performed as described previously.[24] Briefly, MT-4 cells were seeded at 1×10^4 in RPMI 1640 medium containing 10% fetal bovine serum on 12-well plates. The molecular clone of HIV-1_{NL4-3} was used to infect the cells in the presence or absence of diluted peptide inhibitors (sifuvirtide, MT-SFT, C34 or MT-C34). The cells were incubated at 37°C with 5% CO_2 until an extensive cytopathic effect was observed. The culture supernatants were harvested and used for next passage on fresh MT-4 cells with 1.5–2-fold increasing concentrations of peptide. The cells and supernatant were harvested at regular timepoints and stored at −80°C.

Results

The structure of the N-terminal M-T hook-capped SFT

To optimize sifuvirtide, we replaced the N-terminal serine of sifuvirtide by residues methionine (M) and threonine (T), resulting in a novel peptide named MT-SFT (Figure 1). We first performed crystallographic studies to determine whether the incorporated residues adopt the M-T hook structure. As shown in Figure 2(a), MT-SFT formed a typical 6-HB structure with N36 as anticipated. The central N36 trimeric coiled coil is fully wrapped by three MT-SFT peptides in an antiparallel orientation. MT-SFT/N41 also formed a 6-HB structure, regardless that the counterpart of a C-terminal portion of MT-SFT is unavailable on the N41 trimer (Figure 3a).

When performing the molecular replacement using the crystal structure of sifuvirtide (without the M-T hook) as the searching model, the resulting electron-density map showed strong Fo-Fc positive peaks at the N-terminus of sifuvirtide. The positive densities map clearly indicated the shape for a typical M-T hook structure. After manual model building and refinements, we confirmed that the N-terminal residues Met115 and Thr116 adopt the M-T hook structure in both complexes (Figure 2a and b and Figure 3a and b). Briefly, the threonine terminates the α-helical conformation of MT-SFT by rotating its dihedral angle ψ nearly 180°. Consequently, the N-termini of MT-SFT are directed away from the central coiled-coil trimer. The conformation of the threonine is stabilized by an important hydrogen bond between its side-chain hydroxyl group and the backbone NH group of the downstream residues at $i+3$ position (Thr116–Thr119 in MT-SFT/N36, distance: 2.27 Å, angle: 165.3°; Thr116–Thr119 in MT-SFT/N41, distance: 2.76 Å, angle: 165.1°). As the result of the unusual conformation of Thr116, the upstream methionine is then positioned on top of the left side of the hydrophobic pocket on the NHR coiled-coil trimer, so that its hydrophobic side chain can accommodate the hydrophobic groove between the NHR and CHR helices, stabilizing the hydrophobic pocket on the NHR trimer. The N-terminal portions of NHR-bound MT-SFT could be perfectly superimposed on that of CP32, MT-C34 and MT-SC22EK, which contain the M-T hook structure.

The M-T hook greatly enhances the binding of sifuvirtide

Compared with the template peptide C34, the binding affinity of sifuvirtide for the NHR target was markedly enhanced. Thus, it was intriguing to know whether the M-T hook structure can further enhance the binding of sifuvirtide. To this end, we applied CD spectroscopy and ITC experiments. First, the α-helicity and thermostability of the 6-HB core formed by MT-SFT and the NHR-derived peptide N36 were measured by CD spectroscopy in comparison with sifuvirtide and C34-based 6-HBs. The peptide pairs (MT-SFT/N36, sifuvirtide/N36 and C34/N36) were mixed at equal molar concentrations and incubated at 37°C for 30 min. As shown in Figure 4(a), the CD spectra of all three peptide pairs displayed typical double minima at 208 and 222 nm, which indicated the formation of the secondary α-helical structures. The thermostability of each 6-HB, defined as the T_m value, was measured (Figure 4b). Consistently, sifuvirtide-based 6-HB had a significantly increased T_m value (72.2°C) as compared with C34-based 6-HB (65.3°C). Strikingly, the T_m value of MT-SFT-based 6-HB was further increased up to 81.3°C. These results indicated that substitution of the N-terminal residue serine by two M-T hook residues can markedly increase the thermostability of the 6-HB conformation.

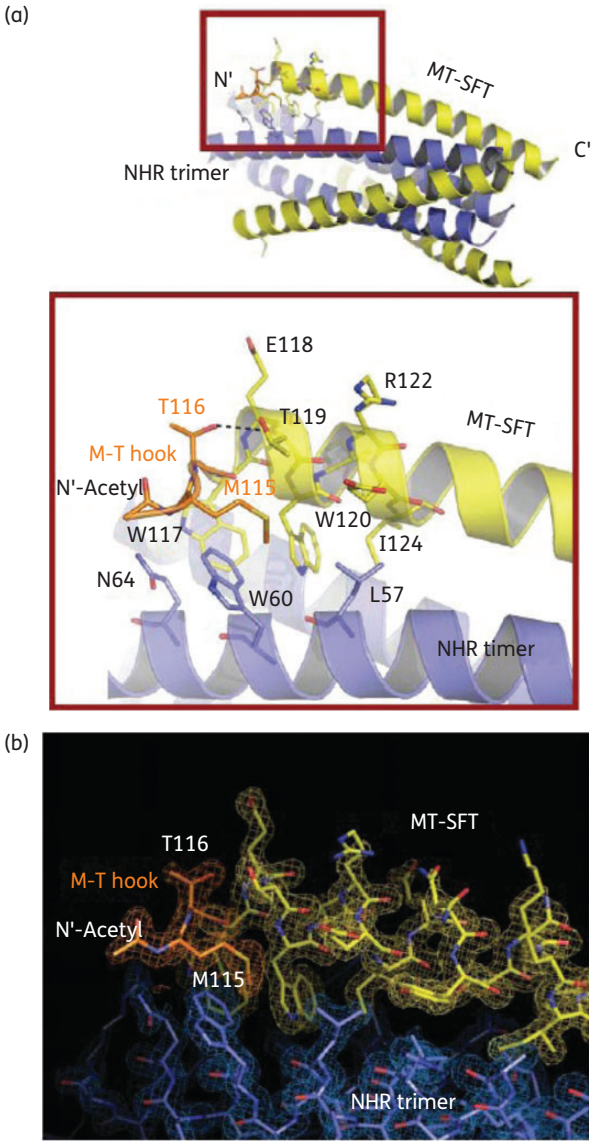

Figure 2. Crystal structure of MT-SFT in complex with N36. (a) Upper part, a ribbon model of the 6-HB structure formed by MT-SFT/N36. The N36 trimer is coloured in blue and the MT-SFT peptides are coloured in yellow. The N-terminus and C-terminus of one peptide are labelled. Lower part, the red boxed portion of the above ribbon model of the 6-HB structure is magnified. Residues Met115 and Thr116 form a hook-like structure (highlighted in orange) that stabilizes the interaction between MT-SFT and the NHR helices. Thr116 terminates the α-helical conformation of the MT-SFT peptide. The hydroxyl group of the Thr116 side chain accepts a hydrogen bond from the NH group of Thr119, directing the N-terminus of MT-SFT away from the central NHR trimer. The side chain of Met115 covers the hydrophobic pocket on the NHR trimer. The M-T hook and residues involved in the interaction with the M-T hook are shown as stick models. The dashed line indicates the hydrogen bond between Thr116 and Thr119. (b) A portion of the 6-HB structure formed by MT-SFT/N36 is displayed as a final stick model with the superimposed final 2Fo-Fc electron-density map (1.5 s contour). The electron density for MT-SFT is shown as a yellow mesh, the electron density for the N-terminal M-T hook is shown as an orange mesh and the electron density for the N36 trimer is shown as a blue mesh. The superimposed stick model is coloured with the same scheme. The key residues forming the M-T hook are labelled.

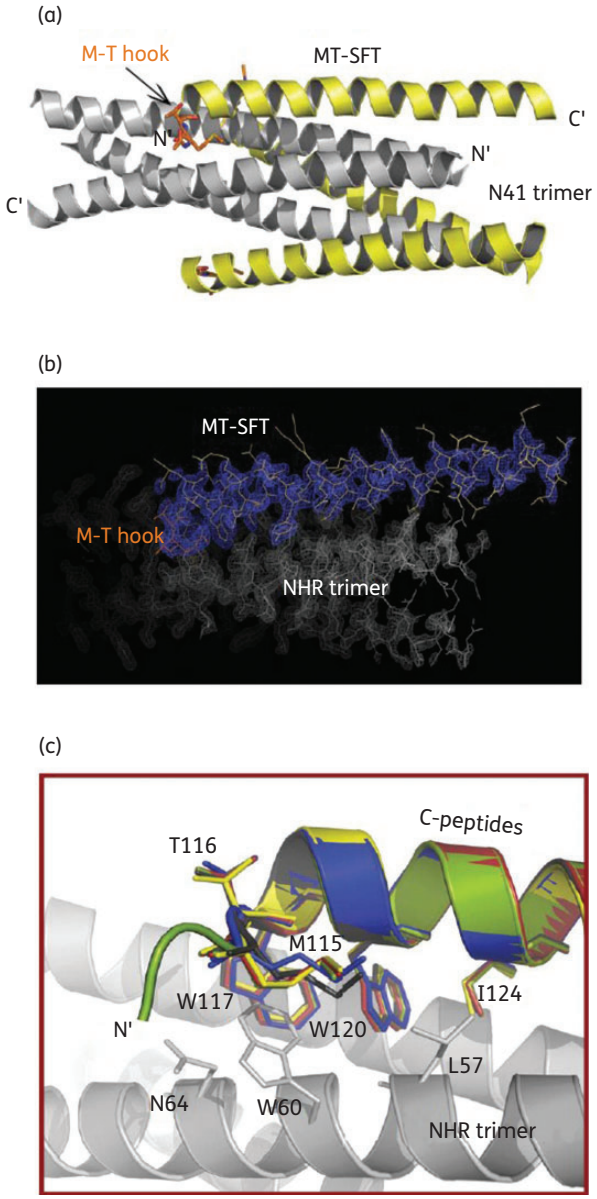

Figure 3. Crystal structure of MT-SFT in complex with N41. (a) A ribbon model of the 6-HB structure formed by MT-SFT/N41. The N41 trimer is coloured in grey and the MT-SFT peptides are coloured in yellow. The N- and C-termini of the peptides are labelled. The M-T hook residues are shown as stick models; they are coloured orange and are labelled. (b) A portion of the 6-HB structure formed by MT-SFT/N41 is displayed as a final atomic model with the superimposed final 2Fo-Fc electron-density map (1.5 s contour). The electron density for N41 is shown in grey and the electron density for MT-SFT is shown in blue. (c) Comparison of the M-T hook structures. The N-terminal portions of N36-bound MT-SFT (yellow), N41-bound MT-SFT (dark grey), CP32 (green), MT-C34 (blue) and MT-SC22EK (red) are superimposed using Coot v0.6. The residues involved in the interaction with the M-T hook are shown as stick models and are labelled. The NHR trimer is coloured in grey.

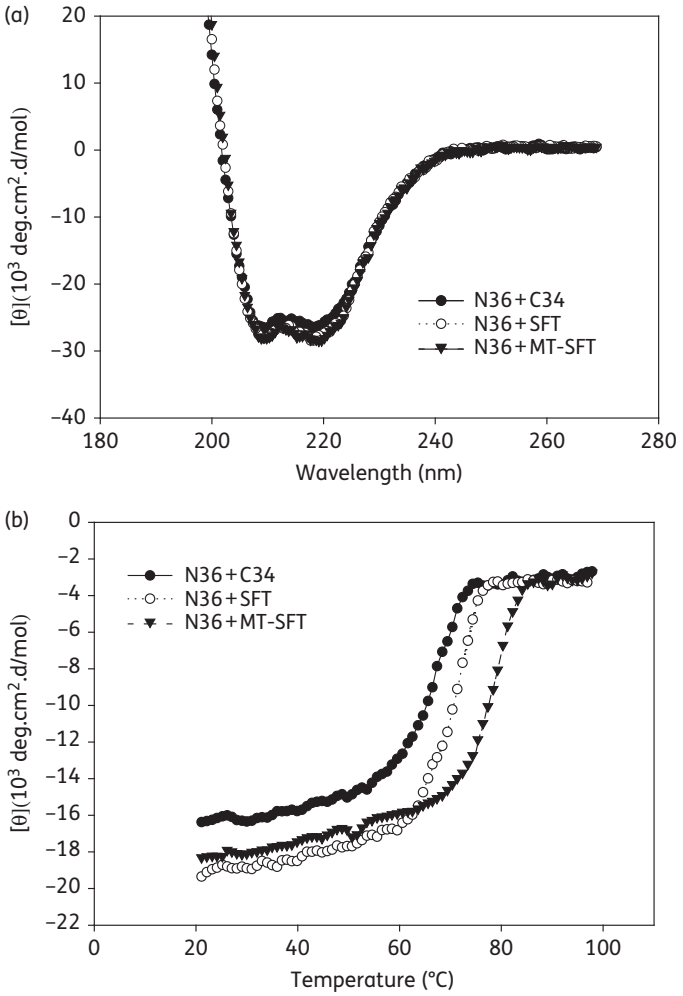

Figure 4. Biophysical characterization of sifuvirtide (SFT) and MT-SFT by CD spectroscopy. The α-helicity (a) and thermostability (b) of the complex formed by N36 and CHR peptides are shown. Final concentration of each peptide in PBS was 10 μM.

We then used the ITC technology to determine the thermodynamic profiles of the molecular interaction between the inhibitors and N36. The heat released or absorbed during the interaction allowed an accurate determination of the binding constant (*K*), reaction stoichiometry (*N*), enthalpy (Δ*H*) and entropy (Δ*S*). As shown in Figure 5, the formation of 6-HBs by sifuvirtide and N36 (Figure 5a) or MT-SFT and N36 (Figure 5b) is a typical enthalpy-driven reaction in which a large amount of heat is released. Compared with sifuvirtide, the *K* value of MT-SFT increased 16.2-fold (from 6.8×10^5 to 1.1×10^7 M^{-1}), suggesting a largely increased binding affinity. Therefore, the M-T hook structure critically determines the interaction of the inhibitors with the NHR target.

The M-T hook greatly improves the antiviral activity of sifuvirtide

Based on our biophysical data, we were interested to compare the anti-HIV activity of sifuvirtide and MT-SFT. In the HIV-1_{NL4-3} Env-mediated cell–cell fusion assay (Figure 6a), sifuvirtide and MT-SFT had IC_{50} values of 3.4 and 1.0 nM, respectively, indicating a 3.4-fold increase of potency for MT-SFT. In the single-cycle entry assay (Figure 6b), sifuvirtide and MT-SFT inhibited HIV-1_{NL4-3}

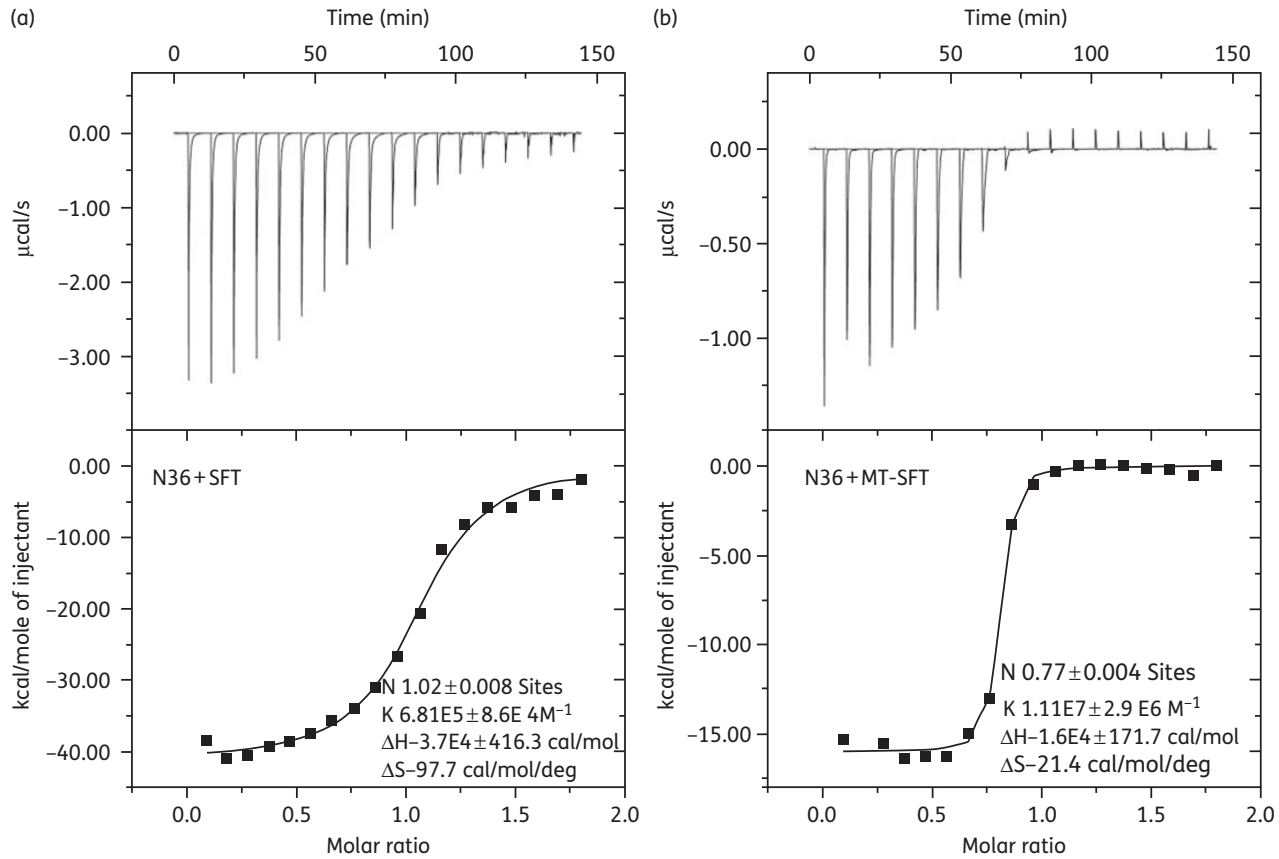

Figure 5. Interaction of sifuvirtide (SFT) and MT-SFT with N36 measured by ITC assay. N36 (1 mM) dissolved in ddH_2O was injected into the chamber containing 100 μM SFT (a) or MT-SFT (b). The experiments were carried out at 25°C. Data acquisition and analysis were performed using MicroCal Origin software (version 7.0).

pseudovirus with IC_{50} values of 3.2 and 0.9 nM, respectively, indicating a 3.6-fold increase. For the wild-type HIV-1_{NL4-3} infection (Figure 6c), sifuvirtide had an IC_{50} of 2.0 nM, whereas MT-SFT had an IC_{50} of 0.6 nM, indicating a 3.3-fold increase. These results demonstrated that the M-T hook residues can enhance the anti-HIV activity of sifuvirtide >3-fold. We also showed that MT-SFT possessed potent inhibitory activity against a panel of primary HIV-1 isolates (Table S2, available as Supplementary data at *JAC* Online). To further understand the mechanism, we compared the inhibitory activity of sifuvirtide and MT-SFT on the formation of the 6-HB structure. As shown in Figure 6(d), sifuvirtide blocked 6-HB formation with an IC_{50} of 0.9 μM, whereas MT-SFT had an IC_{50} value at 0.1 μM. Therefore, we concluded that the M-T hook could confer the inhibitors with high-affinity binding capacity to compete off the viral CHR, and thereby improving the anti-HIV activity.

MT-SFT is a potent inhibitor of drug-resistant HIV-1 variants

We previously found that the M-T hook structure-modified peptides could inhibit drug-resistant HIV-1 variants more efficiently.[28,29] Here, we utilized three panels of HIV-1 mutants to compare sifuvirtide and MT-SFT (Table 1). The Panel 1 and Panel 2 viruses are selected by sifuvirtide and enfuvirtide, respectively, which have been shown to confer high-level cross-resistance. The third panel contains HIV-1 variants carrying naturally occurring mutations in the NHR region that confer a high level of cross-resistance to several potent HIV-1 fusion inhibitors, such as enfuvirtide, T1249 and CP32M. As shown in Table 1, MT-SFT displayed higher potency than sifuvirtide to inhibit various HIV-1 mutants. For example, while sifuvirtide inhibited the Q40H mutant with an IC_{50} of 17.9 nM, MT-SFT had an IC_{50} of 1.9 nM, indicating a 9.4-fold increased potency of MT-SFT. Particularly, while sifuvirtide showed significantly reduced inhibitory activity against HIV-1 strains carrying double mutations (the I37T/N43K and V38A/N42T mutants from Panel 1 and the I37Q/V38M, I37S/V38N and I37V/V38T mutants from the Panel 2), MT-SFT remained highly active. These results verified that the M-T hook can significantly improve the ability of the inhibitors to inhibit drug-resistant HIV-1 variants.

High-affinity binding of MT-SFT to the NHR mutants

To gain insights into the mechanism of the M-T hook-modified inhibitors possessing higher potency against drug-resistant HIV-1 variants, we compared the binding affinity of sifuvirtide and MT-SFT for the NHR mutants. A panel of N36-based peptides carrying single (I37T, V38A, Q40H and N43K) or double (I37T/N43K and V38A/N42T) NHR mutations were synthesized and applied in the CD analysis. As shown in Figure 7, the NHR mutations

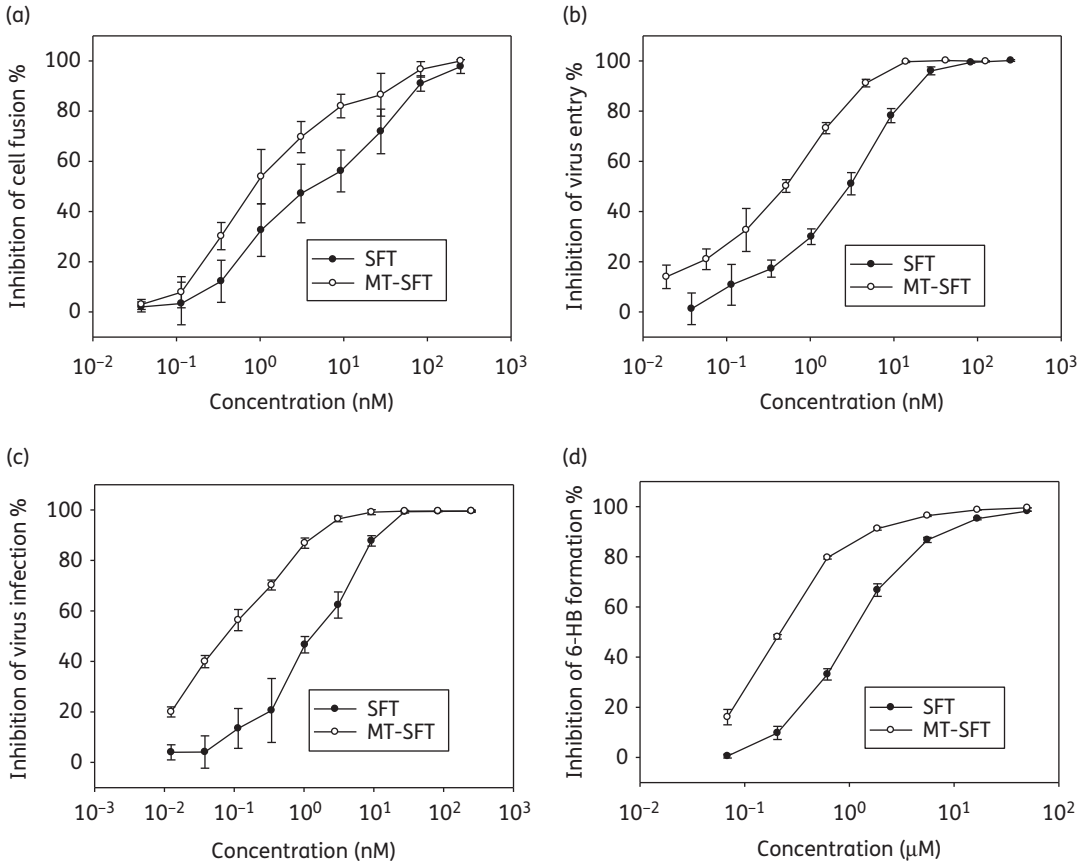

Figure 6. Anti-HIV activity of sifuvirtide (SFT) and MT-SFT peptides. (a) Inhibition of HIV-1_{HXB2} Env-mediated cell fusion. (b) Inhibition of HIV-1_{NL4-3} pseudovirus entry. (c) Inhibition of the wild-type HIV-1_{NL4-3} infection. (d) Inhibition of 6-HB as measured by ELISA. Percentage inhibition of the peptides and IC_{50} values were calculated as described. Data were derived from the results of three independent experiments and are expressed as means ± SD.

could result in a sharp decrease in the thermostability of sifuvirtide-based 6-HBs, such as I37T mutant (T_m = 57.2°C) and Q40H (T_m = 61.2°C); however, the T_m values of MT-SFT-based 6-HBs could be significantly recovered, reaching a degree comparable (I37T, V38A, V38A/N42T) to or greater (Q40H, N43K, I37T/N43K) than that of SFT/N36-based bundle (72.2°C). Therefore, we speculate that the M-T hook structure can compensate the loss of binding affinity in the NHR mutants, thus preserving high activity against sifuvirtide- and enfuvirtide-resistant HIV-1 variants.

The M-T hook significantly increases the genetic barrier to drug resistance

We asked whether the M-T hook structure can confer the inhibitors with a high genetic barrier to developing drug resistance. To address this, we performed a series of passaging experiments to generate virus that was resistant to sifuvirtide or MT-SFT. As shown in Figure 8(a), sifuvirtide-resistant virus was obtained after 38 generations of passaging, at which time the concentration of sifuvirtide reached up to 9600 nM; in sharp contrast, the virus did not acquire obvious resistance to MT-SFT at the same timepoint. We continued an additional 12 passages to select the virus resistant to MT-SFT, leading to a drug concentration of 800 nM. Further, we validated this finding by comparing the peptide pair C34 and MT-C34 in parallel to induce the resistance. Consistently, the virus culture could be reasonably recovered after 38 passages, wherein the concentration of C34 was escalated up to 3200 nM (Figure 8b). Consistently MT-C34 only approached 160 nM due to the difficulty of passaging virus. Therefore, we could conclude that the modified peptide inhibitors possessed an increased genetic barrier to the development of resistance.

Discussion

By solving the crystal structure of the peptide CP32-based 6-HB, we surprisingly identified that the hook-like structure attaches to one side of the NHR pocket tightly, thus stabilizing the NHR-CHR interaction.[27] Using peptides C34 and SC22EK as models, we have demonstrated that the M-T hook conformation could be well preserved at the extreme N-termini of peptides and efficiently strengthened the affinity of NHR–CHR interactions.[28,29] In this study, we incorporated the conserved hook residues in the N-terminus of sifuvirtide and verified again a highly stable M-T hook structure by crystallographic study. MT-SFT was cocrystallized with two different NHR targets, N36 and N41. The N36 trimer can accommodate the entire MT-SFT, whereas the N41 trimer only accommodates the N-terminal part of the inhibitor and leaves ~30% of C-terminal α-helices of MT-SFT overhanging (Figure 3). However, this did not seem to confound the binding of MT-SFT to

Table 1. Inhibitory activity of SFT and MT-SFT against drug-resistant HIV-1 variants

HIV-1_{NL4-3} mutant	IC_{50} (nM)		*n*-fold (i.e. SFT/MT-SFT)	*P* value[a]
	SFT	MT-SFT		
Panel 1				
WT	2.4±0.1	0.8±0.1	3	0.004
I37T	8.4±1.0	2.0±0.3	4.2	<0.001
V38A	8.7±2.1	1.9±0.6	4.6	0.003
V38M	6.2±0.8	1.6±0.3	3.9	<0.001
Q40H	17.9±1.6	1.9±0.7	9.4	<0.001
N43K	13.7±1.7	2.1±0.3	6.5	<0.001
I37T/N43K	244.2±53.1	8.9±0.1	27.4	<0.001
V38A/N42T	120.8±35.8	9.7±1.6	12.5	0.003
Panel 2				
WT	2.4±0.3	0.9±0.1	2.7	<0.001
L33S	6.5±0.4	1.8±0.5	3.6	<0.001
I37Q/V38Q	10.8±2.5	3.0±0.6	3.6	0.003
I37Q/V38M	130.9±48.1	3.3±0.5	39.7	0.013
I37S/V38N	557.2±43.3	20.2±1.7	27.6	<0.001
I37V/V38T	34.5±3.2	2.3±1.1	15	0.004
Panel 3				
L33V	5.3±1.6	1.9±0.6	2.8	0.006
L34M	0.8±0.1	0.2±0.0	4	<0.001
S35F	1.8±0.4	1.1±0.2	1.6	0.025
Q39R	4.6±0.5	1.4±0.1	3.3	<0.001
L54M	2.0±0.6	0.5±0.1	4	0.007
Q56R	19.0±2.0	5.5±1.0	3.5	0.003
Q56K	10.8±2.8	2.0±0.2	5.4	0.003
L54M/Q56K	9.8±4.5	1.5±0.3	6.5	0.016
L54M/Q56R	9.1±1.1	3.9±0.7	2.3	0.001
L34M/L54M/Q56R	7.9±0.6	1.9±0.6	4.2	<0.001

The HIV-1_{NL4-3} pseudoviruses were used for Panel 1 and the molecular clones of HIV-1_{NL4-3} were used for Panels 2 and 3. WT, wild-type virus. The data were derived from the results of three independent experiments and are expressed as means±SD.
[a]Statistical analysis of the IC_{50} values of SFT and MT-SFT by Student's *t*-test.

NHR targets, because both MT-SFT/N36 and MT-SFT/N41 pairs formed stable 6-HB and yielded crystals that were diffracted to high resolution. These data suggest that the crucial region on the NHR is targeted by the N-terminal residues of MT-SFT, in which the M-T hook and PBD play the critical roles. In addition, our findings also suggest a strategy of further optimizing MT-SFT by shortening the peptide from its C-terminus. Although sifuvirtide has already been engineered for high binding, our biophysical data (CD and ITC) indicated that addition of the M-T hook can further fortify the inhibitor binding (Figures 4 and 5). Taken together, we believe that the M-T hook presents a general structural feature when placed at the N-terminus of the PBD of the CHR peptides. It is conceivable that the M-T hook may integrate the PBD, thus synergistically enhancing the interactions of CHR-derived inhibitors with the target NHR sequences.

As the first and only clinically approved HIV-1 fusion inhibitor, enfuvirtide has several prominent disadvantages limiting its wide application.[15,32] First, the antiviral activity of enfuvirtide is generally lower than that of other CHR-derived peptides. Second, it has a short half-life *in vivo*, thus requiring a dosage of 90 mg twice daily. Third, it has a relatively low genetic barrier to induction of drug resistance. The emergence and spread of enfuvirtide-resistant HIV-1 variants resulted in an increased number of patients failing to respond to enfuvirtide treatment. The resistance phenotype is associated mostly with substitutions in amino acids 36–45 of the NHR, with three contiguous residues (Gly36-Ile27-Val38) being a hotspot.[10–12,33,34] To overcome the problem of drug resistance, a number of strategies have been pursued to develop novel peptide inhibitors with significantly improved anti-HIV activity and pharmaceutical profiles.[13–16,21,32] After enfuvirtide, T-1249 was designed as a second-generation fusion inhibitor by adding the PBD at its N-terminus,[35] but its clinical development was discontinued due to formulation difficulties.[36–38] Based on the C34 sequence, more potent peptides were designed by introducing salt bridges that stabilize the helical conformation of the inhibitors, such as sifuvirtide,[22] SC34EK[39] and T2635.[40] Although these new-generation inhibitors were effective against diverse enfuvirtide-resistant HIV-1 strains, they also induced drug-resistant variants.[24,41,42] Previously, the *in vitro* selection of sifuvirtide-resistant HIV-1 variants identified that most of the substitutions were confined to enfuvirtide-resistant positions in the NHR of gp41, including amino acids Ile37, Val38, Gln41 and Asn43 either singly or in combination, and the mutant viruses showed variable degrees of cross-resistance to enfuvirtide.[24]

Our previous studies demonstrated that the M-T hook-capped peptides, such as MT-C34 and MT-SC22EK, had improved activity against T20- and/or sifuvirtide-resistant HIV-1 variants.[28,29] Here, our data show that MT-SFT has significantly improved potency compared with sifuvirtide to block 6-HB formation and inhibit HIV-1 Env-mediated cell fusion, viral entry and infection, but more impressively MT-SFT maintained high potency against a large group of enfuvirtide- and sifuvirtide-resistant viruses, including drug-induced and naturally occurring HIV-1 mutants (Table 1). Consistently, our CD data revealed that MT-SFT interacted with the corresponding NHR mutants with significantly higher stability as compared with sifuvirtide (Figure 7). Nonetheless, the most significant point of this study should be that the M-T hook-modified peptides (MT-SFT and MT-C34) had a considerably higher genetic barrier to developing drug resistance. During *in vitro* selection, the escalating concentrations of the peptides sifuvirtide and C34 were able to easily select resistant viruses, in agreement with previous studies.[24,43] In a sharp contrast, the addition of the M-T hook residues (MT-SFT and MT-C34) markedly changed the resistance profiles (Figure 8). We have also found that the M-T hook-modified short-peptide inhibitor MT-SC22EK behaved with a similar phenotype (H. Chong, Z. Qiu, J. Sun, Y. Qiao and Y. He, unpublished data). Taken together, we consider that the M-T hook structure can endow the peptide fusion inhibitors with a high genetic barrier to developing resistant HIV-1 variants, which provides an important feature for drug development. Recently, Eggink *et al.*[44] described four mechanisms of drug resistance, including reduced contact, steric obstruction, electrostatic repulsion and electrostatic attraction. Our studies on the sifuvirtide resistance profile could deduce several additional mechanisms, such as hydrogen bond disruption and hydrophobic contact disruption.[23,24] It is highly interesting to know how the M-T hook structure changes the

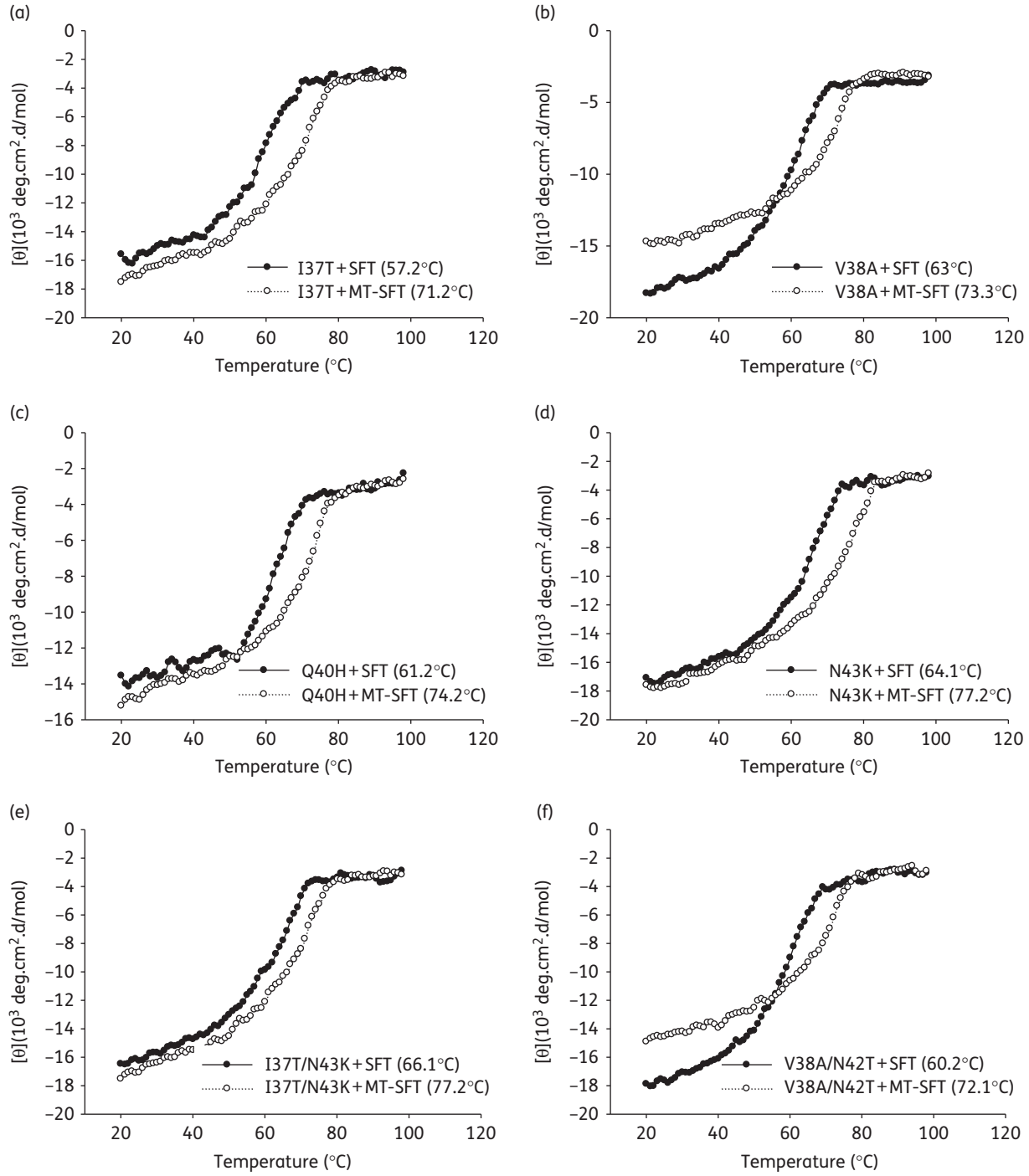

Figure 7. Binding stability of sifuvirtide (SFT) and MT-SFT with N36 mutants determined by CD spectroscopy. (a) I37T, (b) V38A, (c) Q40H, (d) N43K, (e) I37T/N43K and (f) V38A/N42T. Final concentration of each peptide in PBS was 10 μM.

resistance profiles of sifuvirtide and C34. From our structural studies, we could see that M-T hook binds the NHR target in a rather unique way compared with any other region of the peptide. Instead of binding to the groove between two adjacent NHR helices, the M-T hook binds to the side of the hydrophobic pocket as well as the residues on its own PBD region. Therefore, it seems that the M-T hook serves to strengthen the PBD–pocket interaction rather than target novel sites on the NHR trimer. It is well characterized that residues involving PBD–pocket interaction are the most conserved residues during HIV-1 evolution; the mutation of these residues is often lethal to the virus. Thus, the balance between virus survival and drug resistance becomes hard to maintain and the genetic barrier to drug resistance against the M-T hook increases. Although MT-SFT and MT-C34 are currently

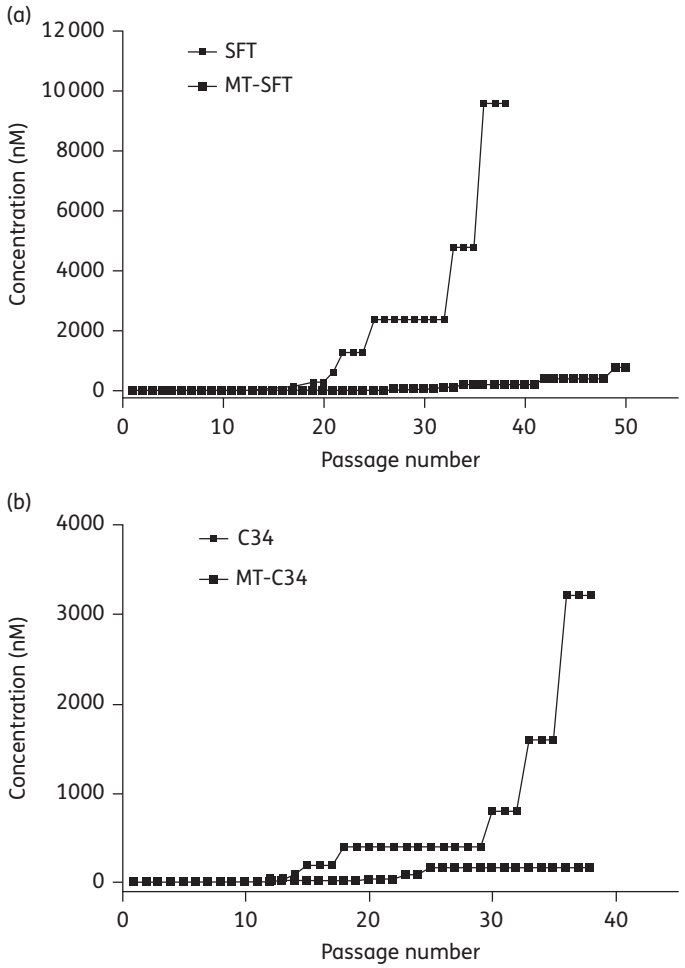

Figure 8. *In vitro* selection of HIV-1 resistant to fusion inhibitors. (a) Induction of sifuvirtide (SFT)- and MT-SFT-resistant HIV-1. (b) Induction of C34- and MT-C34-resistant HIV-1. The molecular clone of HIV-1_{NL4-3} was passaged in the presence of 1.5–2-fold escalating concentrations of peptides.

undergoing a delayed selection procedure, they may be gradually escalated to higher concentrations thus resulting in the high-level resistant HIV-1 mutants. We expect to explore the mechanism of HIV-1 resistance to the M-T hook-based peptides by multiple approaches, which would be helpful for understanding the mechanisms of HIV-1 fusion and for designing novel fusion inhibitors.

In conclusion, the significance of our studies includes three aspects. First, we have verified that the M-T hook structure is a general feature of CHR-derived inhibitors. Second, the M-T hook structure plays a vital role for designing fusion inhibitors against enfuvirtide- and sifuvirtide-resistant HIV-1 mutants. Third, the M-T hook-based HIV-1 fusion inhibitors have a high genetic barrier to developing drug resistance.

Funding

This work was supported by grants from the National Science Foundation of China (81025009, 81271830) and National 973 Program of China (2010CB530100).

Transparency declarations

None to declare.

Supplementary data

Tables S1 and S2 are available as Supplementary data at *JAC* Online (http://jac.oxfordjournals.org/).

References

1 Flexner C. HIV drug development: the next 25 years. *Nat Rev Drug Discov* 2007; **6**: 959–66.

2 Engelman A, Cherepanov P. The structural biology of HIV-1: mechanistic and therapeutic insights. *Nat Rev Microbiol* 2012; **10**: 279–90.

3 Este JA, Telenti A. HIV entry inhibitors. *Lancet* 2007; **370**: 81–8.

4 Lobritz MA, Ratcliff AN, Arts EJ. HIV-1 entry, inhibitors, and resistance. *Viruses* 2010; **2**: 1069–105.

5 Gulick RM, Lalezari J, Goodrich J *et al*. Maraviroc for previously treated patients with R5 HIV-1 infection. *N Engl J Med* 2008; **359**: 1429–41.

6 Fatkenheuer G, Nelson M, Lazzarin A *et al*. Subgroup analyses of maraviroc in previously treated R5 HIV-1 infection. *N Engl J Med* 2008; **359**: 1442–55.

7 Kilby JM, Hopkins S, Venetta TM *et al*. Potent suppression of HIV-1 replication in humans by T-20, a peptide inhibitor of gp41-mediated virus entry. *Nat Med* 1998; **4**: 1302–7.

8 Lalezari JP, Henry K, O'Hearn M *et al*. Enfuvirtide, an HIV-1 fusion inhibitor, for drug-resistant HIV infection in North and South America. *N Engl J Med* 2003; **348**: 2175–85.

9 Wild CT, Shugars DC, Greenwell TK *et al*. Peptides corresponding to a predictive α-helical domain of human immunodeficiency virus type 1 gp41 are potent inhibitors of virus infection. *Proc Natl Acad Sci USA* 1994; **91**: 9770–4.

10 Rimsky LT, Shugars DC, Matthews TJ. Determinants of human immunodeficiency virus type 1 resistance to gp41-derived inhibitory peptides. *J Virol* 1998; **72**: 986–93.

11 Baldwin CE, Sanders RW, Deng Y *et al*. Emergence of a drug-dependent human immunodeficiency virus type 1 variant during therapy with the T20 fusion inhibitor. *J Virol* 2004; **78**: 12428–37.

12 Greenberg ML, Cammack N. Resistance to enfuvirtide, the first HIV fusion inhibitor. *J Antimicrob Chemother* 2004; **54**: 333–40.

13 Berkhout B, Eggink D, Sanders RW. Is there a future for antiviral fusion inhibitors? *Curr Opin Virol* 2012; **2**: 50–9.

14 Naider F, Anglister J. Peptides in the treatment of AIDS. *Curr Opin Struct Biol* 2009; **19**: 473–82.

15 Eggink D, Berkhout B, Sanders RW. Inhibition of HIV-1 by fusion inhibitors. *Curr Pharm Des* 2010; **16**: 3716–28.

16 He Y. Synthesized peptide inhibitors of HIV-1 gp41-dependent membrane fusion. *Curr Pharm Des* 2013; **19**: 1800–9.

17 Chan DC, Fass D, Berger JM *et al*. Core structure of gp41 from the HIV envelope glycoprotein. *Cell* 1997; **89**: 263–73.

18 Lu M, Kim PS. A trimeric structural subdomain of the HIV-1 transmembrane glycoprotein. *J Biomol Struct Dyn* 1997; **15**: 465–71.

19 Tan K, Liu J, Wang J *et al*. Atomic structure of a thermostable subdomain of HIV-1 gp41. *Proc Natl Acad Sci USA* 1997; **94**: 12303–8.

20 Weissenhorn W, Dessen A, Harrison SC *et al*. Atomic structure of the ectodomain from HIV-1 gp41. *Nature* 1997; **387**: 426–30.

21 Steffen I, Pohlmann S. Peptide-based inhibitors of the HIV envelope protein and other class I viral fusion proteins. *Curr Pharm Des* 2010; **16**: 1143–58.

22 He Y, Xiao Y, Song H *et al*. Design and evaluation of sifuvirtide, a novel HIV-1 fusion inhibitor. *J Biol Chem* 2008; **283**: 11126–34.

23 Yao X, Chong H, Zhang C *et al*. Broad antiviral activity and crystal structure of HIV-1 fusion inhibitor sifuvirtide. *J Biol Chem* 2012; **287**: 6788–96.

24 Liu Z, Shan M, Li L *et al*. In vitro selection and characterization of HIV-1 variants with increased resistance to sifuvirtide, a novel HIV-1 fusion inhibitor. *J Biol Chem* 2011; **286**: 3277–87.

25 He Y, Cheng J, Li J *et al*. Identification of a critical motif for the human immunodeficiency virus type 1 (HIV-1) gp41 core structure: implications for designing novel anti-HIV fusion inhibitors. *J Virol* 2008; **82**: 6349–58.

26 He Y, Cheng J, Lu H *et al*. Potent HIV fusion inhibitors against enfuvirtide-resistant HIV-1 strains. *Proc Natl Acad Sci USA* 2008; **105**: 16332–7.

27 Chong H, Yao X, Qiu Z *et al*. Discovery of critical residues for viral entry and inhibition through structural insight of HIV-1 fusion inhibitor CP621-652. *J Biol Chem* 2012; **287**: 20281–9.

28 Chong H, Yao X, Sun J *et al*. The M-T hook structure is critical for design of HIV-1 fusion inhibitors. *J Biol Chem* 2012; **287**: 34558–68.

29 Chong H, Yao X, Qiu Z *et al*. Short-peptide fusion inhibitors with high potency against wild-type and enfuvirtide-resistant HIV-1. *FASEB J* 2013; **27**: 1203–13.

30 He Y, Liu S, Li J *et al*. Conserved salt bridge between the N- and C-terminal heptad repeat regions of the human immunodeficiency virus type 1 gp41 core structure is critical for virus entry and inhibition. *J Virol* 2008; **82**: 11129–39.

31 Chong H, Yao X, Zhang C *et al*. Biophysical property and broad anti-HIV activity of albuvirtide, a 3-maleimimidopropionic acid-modified peptide fusion inhibitor. *PLoS One* 2012; **7**: e32599.

32 Berkhout B, Sanders RW. Molecular strategies to design an escape-proof antiviral therapy. *Antiviral Res* 2011; **92**: 7–14.

33 Mink M, Mosier SM, Janumpalli S *et al*. Impact of human immunodeficiency virus type 1 gp41 amino acid substitutions selected during enfuvirtide treatment on gp41 binding and antiviral potency of enfuvirtide in vitro. *J Virol* 2005; **79**: 12447–54.

34 Sista PR, Melby T, Davison D *et al*. Characterization of determinants of genotypic and phenotypic resistance to enfuvirtide in baseline and on-treatment HIV-1 isolates. *AIDS* 2004; **18**: 1787–94.

35 Eron JJ, Gulick RM, Bartlett JA *et al*. Short-term safety and antiretroviral activity of T-1249, a second-generation fusion inhibitor of HIV. *J Infect Dis* 2004; **189**: 1075–83.

36 Martin-Carbonero L. Discontinuation of the clinical development of fusion inhibitor T-1249. *AIDS Rev* 2004; **6**: 61.

37 Melby T, Demasi R, Cammack N *et al*. Evolution of genotypic and phenotypic resistance during chronic treatment with the fusion inhibitor T-1249. *AIDS Res Hum Retroviruses* 2007; **23**: 1366–73.

38 Eggink D, Baldwin CE, Deng Y *et al*. Selection of T1249-resistant human immunodeficiency virus type 1 variants. *J Virol* 2008; **82**: 6678–88.

39 Nishikawa H, Nakamura S, Kodama E *et al*. Electrostatically constrained α-helical peptide inhibits replication of HIV-1 resistant to enfuvirtide. *Int J Biochem Cell Biol* 2009; **41**: 891–9.

40 Dwyer JJ, Wilson KL, Davison DK *et al*. Design of helical, oligomeric HIV-1 fusion inhibitor peptides with potent activity against enfuvirtide-resistant virus. *Proc Natl Acad Sci USA* 2007; **104**: 12772–7.

41 Eggink D, Bontjer I, Langedijk JP *et al*. Resistance of human immunodeficiency virus type 1 to a third-generation fusion inhibitor requires multiple mutations in gp41 and is accompanied by a dramatic loss of gp41 function. *J Virol* 2011; **85**: 10785–97.

42 Shimura K, Nameki D, Kajiwara K *et al*. Resistance profiles of novel electrostatically constrained HIV-1 fusion inhibitors. *J Biol Chem* 2010; **285**: 39471–80.

43 Nameki D, Kodama E, Ikeuchi M *et al*. Mutations conferring resistance to human immunodeficiency virus type 1 fusion inhibitors are restricted by gp41 and Rev-responsive element functions. *J Virol* 2005; **79**: 764–70.

44 Eggink D, Langedijk JP, Bonvin AM *et al*. Detailed mechanistic insights into HIV-1 sensitivity to three generations of fusion inhibitors. *J Biol Chem* 2009; **284**: 26941–50.